"Hallucinating Irises" – Dealing with Partial & Occluded Iris Regions

Taihei Munemoto, Yung-hui Li, and Marios Savvides
Electrical and Computer Engineering, Carnegie Mellon University, 5000 Forbes Ave, Pittsburgh PA 15213

***Abstract*—In this paper, we examine a novel image-filling algorithm to fill the occluded and partial regions of the iris. In iris recognition, these occlusions naturally appear due to eyelids being partially closed, eye movements and eye-lashes. Additionally, specular reflections arising from the iris-camera illuminator are present and produce occlusion artifacts on the iris region. In the polar representation of iris images, additional 'nuisance' parameters include image regions containing the pupil and sclera due to inaccurate iris segmentations. Thus, for accurate iris recognition, it is important to reduce the effect of these nuisance parameters so that the performance of the iris recognition system can be maximized. Typically, a mask region (automatic or manual) is defined to ignore occluded or affected iris regions from such nuisance artifacts. However, in the feature extraction stage, especially using Gabor type extraction, the features near the edge of these artifacts are also affected due to the tail supports of these filters that overflow on occluded irises. We propose a novel method for filling in the occluded regions by synthesizing the iris pattern from this current exemplar image and show that a significant improvement on the Iris Challenge Evaluation (ICE) dataset can be made.**

I. Introduction

IRIS identification is regarded as a reliable biometric system for identification and authentication, and therefore, has been intensively studied for over a decade. There are advantages to using iris patterns as a biometric modality. One of the advantages is that the iris remains relatively stable over a lifetime. Another advantage is that the iris pattern is known to have statistical independence for each person, or even each eye. One of the early successes of iris recognition algorithms was shown in the work of J. Daugman [1]. He applied a complex two dimensional Gabor filter to normalized iris images and created binary maps by encoding the phase of complex valued filter responses. Other successful algorithms by Wildes [2], and Boles [3] also show the robustness of iris patterns for human verification and identification.

While many proposed algorithms are shown to be successful in particular iris databases prepared in relatively controlled environments, there are also limitations. This is due to several factors, such as occlusions, poor focus of images, and inconsistent camera angles. Occlusions occur especially frequently because it is natural for a person's eyes to be covered by the eyelids and eyelashes. Also, specular reflections appear in the iris image due to illumination while the eye images are captured. The pupil and sclera may also appear in the polar representation of an iris image because of inaccurate iris segmentation. An example of noises in an iris image is shown in Figure. 1. If an eye image database is taken under the condition that these noises appear on the captured iris images, frequently, it is difficult to properly identify/verify an individual.

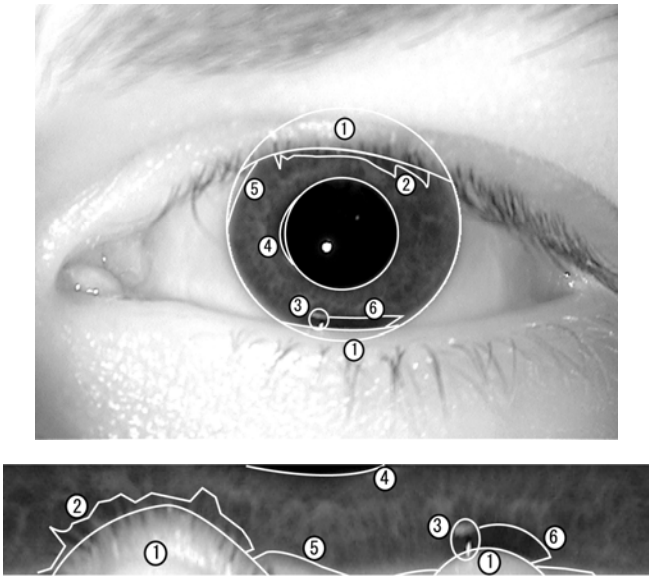

Fig. 1. Top: Occluded iris regions found in Cartesian domain. The numbers in this figure correspond to, 1) eyelids, 2) eyelashes, 3) specular reflections, 4) pupil, 5) sclera, and 6) shadow caused by an eyelid. Bottom: Iris occlusion regions found in polar domain. The numbers in the bottom figure correspond to the noise types in the top figure.

In one of the most common frameworks of the iris recognition system, an iris image is unwrapped to polar representation and linearly filtered by using Gabor filters for feature extraction and occluded regions are detected and excluded by using a mask. In this framework, it is important to not only exclude the noise region, but also estimate the true texture patterns behind these occlusions. Even though masks are used for comparison of iris features, the features around masks are still affected by noise. This is because the response of filters near the boundary of the mask is affected by the noisy pixels.

In our work, we focused on reducing these noises in the polar representation of iris images. Given an iris image and a mask, we applied an image-filling algorithm to estimate the texture pattern inside the occluded iris region. We tested the image-filling algorithm proposed by Criminisi et al. [4], where the masked regions are filled with texture patterns from a non-occluded iris region within the same iris image. A detailed description of the algorithm is given in Section III.

The rest of this paper is organized as follows. Section II describes the related work for noise removal of iris images. Section III describes the image-filling algorithm that we applied. Section IV explains the experimental details and results. Finally, conclusions are given in Section V.

II. Related Work

So far, there are several papers that focus on noise and occlusion removal on iris images in either the Cartesian domain or polar domain. While some proposed algorithms only exclude the noisy regions in an iris image, others estimate the texture patterns behind these regions found on iris images.

Kong and Zhang [5] proposed modeling two types of eyelashes, separable eyelashes and multiple eyelashes. To detect separable eyelashes, he used a one-dimensional Gabor filter. He located separable eyelashes by thresholding the results of convolution of iris images (in Cartesian domain) and the filter. To detect multiple eyelashes, he used the variance of a 5×5 window. If the window was located where a lot of eyelashes overlapped, the variance of the intensity within the window was smaller. Thus, he found a way to detect multiple eyelashes by simply thresholding the variance. It is important to note that his method has not been tested on a large open iris database. It is still unknown if his method performs well on the common benchmarking iris database such as NIST ICE database [10].

Huang et al. [6] proposed the use of phase congruency. He used a bank of two-dimensional Log-Gabor filters to obtain phase congruency, and then used it in the criterion function to detect noises in iris images. After finding the noise regions, he filled the regions with the image-filling algorithm described in [7].

Zhang et al. [8] proposed an eyelash removal algorithm. In his method, first the magnitude and direction of gradient are calculated for all pixels in an iris image by approximating the partial derivatives with Sobel operators. Then, for each pixel with its gradient magnitude higher than a threshold, the variance of gradient magnitude within a window of size $m \times n$ centered at the pixel is calculated. If eyelashes are present within the window, the gradient direction in the window is strong in one direction. Therefore, the eyelashes can be found by thresholding the variance of gradient directions. After eyelashes are detected, the one-dimensional median filtering is applied to fill in these eyelashes.

III. Image-filling Algorithm

In this section, the image-filling algorithm proposed by Criminisi et al. [4] is described. Given an iris image with occlusions, this algorithm estimates the texture pattern behind the occlusions by taking sample patterns from a non-occluded area in the same iris image. This algorithm is designed to preserve the textures of the image as well as the boundaries of different textures.

A. Notations and Definitions of Regions and Points

First, noise regions to be removed, Ω, are defined. In our framework, the noise regions are the eyelid, eyelashes, specular reflections, pupil, sclera, and shadows of eyelids on iris images. For all images in a database, we created masks in two ways: 1) manually and 2) by using the algorithms proposed by Libor Masek [9]. While masks created manually completely cover all occluded regions in the iris images, the masks created by Masek's algorithms contain errors. His method only excludes eyelashes and eyelids, and is less accurate in comparison to the manually created mask as the algorithm performs the linear Hough transform to find eyelids and uses simple thresholding for eyelashes. The goal of this paper is to examine the effect of recovering the texture of occluded regions and mitigating the effect of feature extraction at these boundaries.

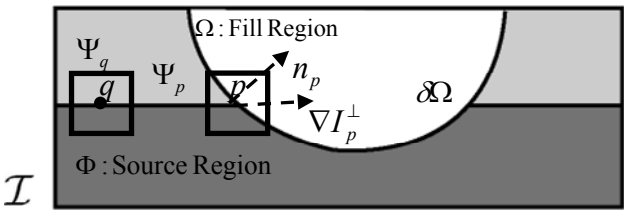

Fig. 2: The notations diagrams. The noise region is denoted as Ω, and its contour is denoted as δΩ. The vector n_p is orthogonal to the contour δΩ. Ψ_p is a window taken from the noise region, centered at p, and Ψ_q is a window taken from source region, centered at q. $\nabla I_p^{\perp}$ is a gradient vector at point p.

We also define the source region Φ. From this region, we take sample windows to place them into noise regions, Ω. In our implementation, we define the source regions as an entire non-occluded region in an iris image that is $\Phi = \mathcal{I} - \Omega$, where $\mathcal{I}$ is the entire image. We can also choose the source region as dilated regions of masks, yet in this experiment, it is out of our focus.

Other notations are as follows. We define the size of template window Ψ_a, where the subscript "a" defines the center of the window. We choose a 9×9 window size as Criminisi did in [4]. We use δΩ for the contour of noise regions, and n_p as a unit vector orthogonal to the contour line at point p, where p lies on the contour line $(p \in \delta\Omega)$. Point q is a point that lies in the source regions $\Phi\,(q \in \Phi)$. These notations are illustrated in Figure. 2.

Given these defined regions and points, the algorithm iterates three steps to fill in the noise regions. These steps are 1) computing priority for the order of filling process, 2) filling the noise region with a patch from source region, and 3) updating priority values. The algorithm repeats these three steps until it fills all noise regions in the given image. These steps are explained in detail below (Also, the block diagram for these steps is described in Figure. 3).

B. Computing Priorities

To fill the region in a way we can preserve the structure of the original image, the order of filling is important. So, for each pixel on the contour of the noise region $p \in \delta\Omega$, a priority function $P(p)$ is calculated as the multiplication of

two values:

$$P(p) = C(p)D(p) \quad (1)$$

$C(p)$ is called confidence term and $D(p)$ is called data term. These values are defined as the follows:

$$C(p) = \frac{\sum_{q \in \Psi_p \cap \Phi} C(q)}{|\Psi_p|}, \quad D(p) = \frac{\left|\nabla I_p^{\perp} \cdot n_p\right|}{\alpha} \quad (2)$$

where $|\Psi_p|$ is the area of Ψ_p, α is a normalization constant set to 255, and $\nabla I_p^{\perp}$ is a gradient vector (a vector whose components are the partial derivatives with respect to x and y directions) rotated 90 degrees.

The intuition behind the confidence term $C(p)$ is that the term gives preference to a point on the contour whose window contains less unknown values. For example, if a window centered at a noise pixel contains only the noise pixel, the confidence value at the noise pixel is high ($C(p)$ is close to 1). As a result, this term weights the priority term so that the priority of filling to be roughly concentric order. Initially, the confidence term $C(p)$ is set to zero for the noise region, and one for the source region.

The data term $D(p)$ describes how strong the edge of different texture hitting the contour of occluded regions $\delta\Omega$ is. The data term is the inner product of two unit vectors. One of the vectors is the unit vector whose direction is orthogonal to the gradient orientation at the pixel, and the other is the unit vector whose direction is normal to the contour of noise region Ω. If, at a pixel, a strong edge of two textures is hitting the contour of the occluded region orthogonally, the data term is high for that pixel. The data term is necessary for preserving the boundary of different iris textures.

After computing $P(p)$ around the contour of the noise region we get a point $\hat{p}$ which has the maximum priority $P(\hat{p})$.

C. *Searching the Best Window*

After computing the point with the maximum priority, $\hat{p}$, we select a window, $\Psi_{\hat{p}}$, around this point. Within this window, occluded pixels are chosen to be filled in. In this step, we find a window $\Psi_{\hat{q}}$, which is a window centered at a point $\hat{q}$ in the source region. To find $\hat{q}$, we search the points in the source region that are $q \in \Phi$ with the following criteria function

$$\Psi_{\hat{q}} = \arg\min_{\Psi_q \in \Phi} d(\Psi_{\hat{p}}, \Psi_q) \quad (3)$$

where the distance function $d(\Psi_{\hat{p}}, \Psi_q)$ is the sum of squared difference (SSD) between the known pixels in window $\Psi_{\hat{p}}$ and corresponding pixels in Ψ_q. After finding the best window $\Psi_{\hat{q}}$, the corresponding pixels are copied into the noise pixels in window $\Psi_{\hat{p}}$.

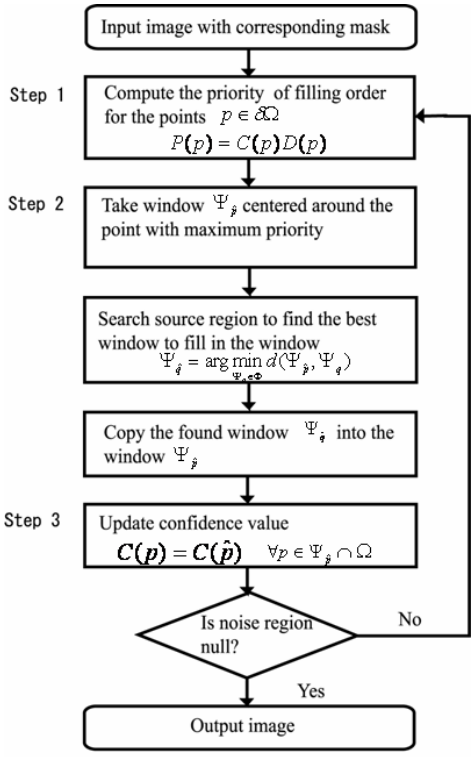

Fig. 3: The block diagram of the image-filling algorithm

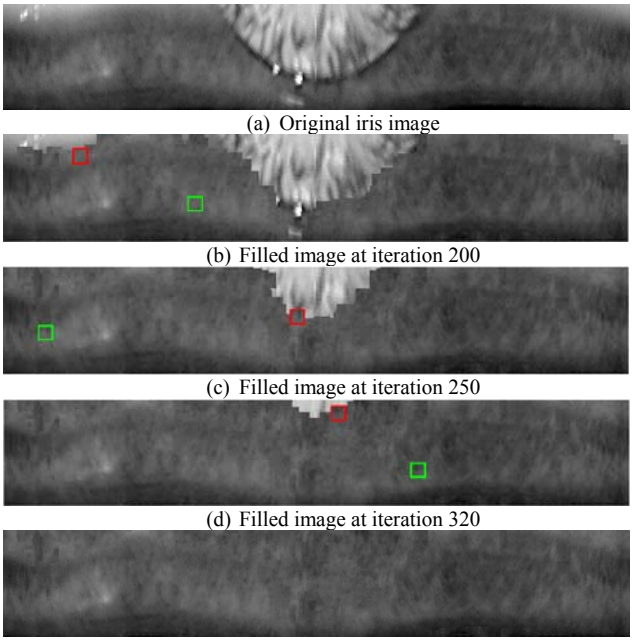

(a) Original iris image

(b) Filled image at iteration 200

(c) Filled image at iteration 250

(d) Filled image at iteration 320

(e) "Hallucinated Iris image" whose occlusions are completely filled

Fig. 4: Iris image filling process. The green box in Figure 4b-4d shows the sample texture patterns copied. The red box in Figure. 4b-4d shows the occlusion region filled with the sample texture patterns from the same iris.

D. *Updating Confidence Values*

After $\Psi_{\hat{q}}$ is copied into $\Psi_{\hat{p}}$, the confidence term $C(p)$ is updated according to the following criteria:

$$C(p) = C(\hat{p}) \quad (4)$$

Where $\forall p \in \Psi_{\hat{p}} \cap \Omega$. Therefore, priority values around the contour of the noise region $\delta\Omega$ are also updated. These three steps are iterated until all pixels in the fill region $\delta\Omega$ are replaced with the patch taken from source region Φ. The example images for this process are shown in Figure 4.

IV. Experimental Setting and Results

A. Baseline Algorithms

We have tested the performance of our algorithm by using Libor Masek's [9] feature encoding and matching algorithm, a public implementation of interpretation of Daugman's algorithm[1] which has become a standard in benchmarking iris performance improvements in the field. One advantage is that the MATLAB code is publicly available and, therefore, widely tested and benchmarked in many papers.

In summary, Masek's implementation extracts features from the polar representation of iris images by convolving them with the one-dimensional complex Log-Gabor filter, row by row. As in Daugman's algorithm, the phase information at each pixel location is quantized into two bits of binary information. When we compare two different iris codes, the Hamming distance is calculated to find the similarity of these codes.

In the feature encoding process, the only difference between Daugman's algorithm and Masek's algorithm is that Daugman uses a complex two-dimensional Gabor filter whereas Masek uses a complex 1D Log-Gabor filter.

B. Dataset

We conducted our research on NIST Iris Challenge Evaluation (ICE) database [10]. The ICE database includes left and right eyes from test subjects. In our experiment we use the left-eye dataset, which contains 1528 images from 120 different classes. The image size is 640×480, and these images are segmented and unwrapped so that the iris is represented in the polar domain.

From the left eyes in the ICE database, we created two iris datasets using two different segmentation algorithms. One algorithm is proposed by Masek [9]. His segmentation scheme assumes that the inner and outer boundary of the iris is a non-concentric circle. We also use another segmentation method proposed by [11], which we name CMU-1.

For the dataset processed by Masek's algorithm, we observed that the segmentation results of the 133 images are extremely inaccurate. Therefore, we excluded these images in our testing. We only used 1395 iris images out of the 1528 ICE left-eye images (91.3%). For the dataset processed by CMU-1 algorithm, we used all the images as CMU segmented could handle all the images. The number of intra-class comparisons (authentic) is 12512 for the dataset created by Masek's algorithm and 14653 for the dataset created by CMU-1 algorithm. The number of inter-class comparisons (imposter) is 959,803 for the dataset created by

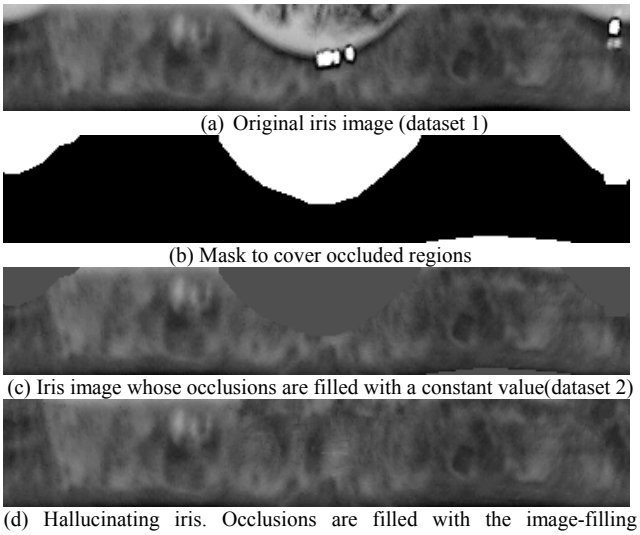

(a) Original iris image (dataset 1)

(b) Mask to cover occluded regions

(c) Iris image whose occlusions are filled with a constant value(dataset 2)

(d) Hallucinating iris. Occlusions are filled with the image-filling algorithm (dataset 3)

Fig. 5: Example iris images from iris images segmented by CMU-1 algorithm. (a) Original iris image in polar domain. (b) Manually created mask for the original image. (c) Iris image whose masked region is filled with the mean value of non-masked region in the same image. This is same as the Masek's algorithm. (d) Iris image whose masked region is filled with the image filling algorithm described in Section III

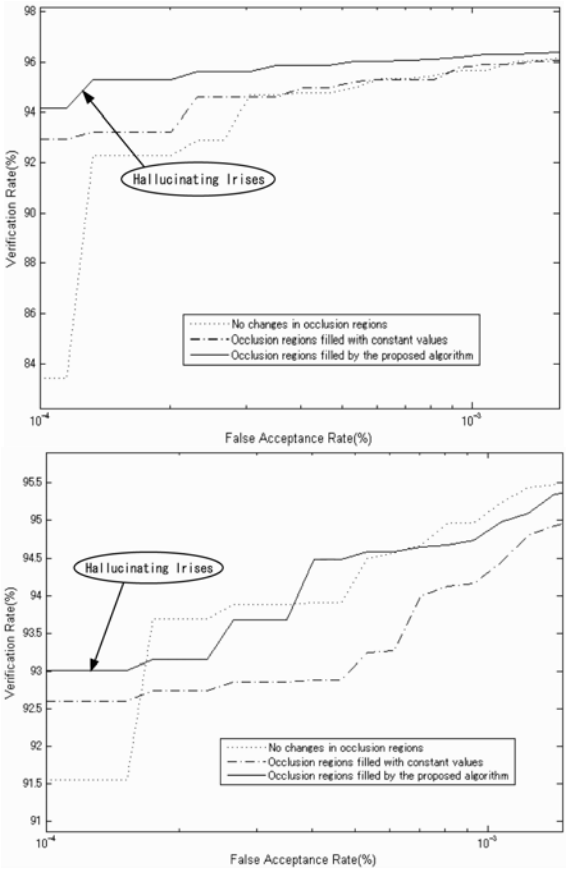

Fig. 6. Top: ROC curves for iris images segmented by CMU-1 algorithm. Bottom: ROC curves for iris images segmented by Masek's algorithm

Masek's algorithm and 1,151,975 for the dataset created by CMU-1 algorithm.

As we discussed in the previous section, we created two types of masks to cover the occluded regions in the iris images in the polar domain. For the iris dataset created by Masek's algorithm, we used masks created by his method. For the iris dataset created by CMU-1 algorithm, we used manually created masks.

Given two datasets created by different segmentation algorithms, we created 6 sets of different features. For each dataset, we obtained features (iris codes) by encoding 1) original iris images, 2) iris images whose masked regions are replaced with the mean values of non-masked regions, and 3) iris images whose masked regions are replaced with the intensity values found by the image-filling algorithm. An example of these images is shown in Figure 4 (segmented by CMU-1 algorithm). The iris images shown in Figure 5 are encoded by our baseline algorithms.

C. Results

The Receiver Operating Characteristic curve (ROC curve) is shown in the Figure 6. For both top and bottom ROCs in Figure 6, we observed that using the dataset whose occluded regions are filled with our algorithm results in a lower False Reject Rate (FRR) or higher Verification Rate (VR), especially when the False Accept Rate (FAR) is required to be small. In Figure 6 top ROC, we can see that at a FAR of 0.0001%, the FRR is reduced by more than 10% (VR is increased by 10%). In contrast, in Figure 6 bottom ROC, we observed that the FAR reduced slightly (1.5%). This is because the mask created by Masek's algorithm is inaccurate, causing the image filling algorithm to replicate the incorrect iris sample patterns into the mask regions and use incorrect regions for matching. The results are also summarized in the Table 1. The example iris images whose noise regions are filled with the filling algorithm is in Figure 7 and Figure 8. In Figure 7, the iris images are segmented by CMU-1 algorithm and masks are created manually. In Figure 8, the iris images are segmented by Masek's algorithm and masks are also generated by his algorithm.

Table 1: False Reject Rate at False Acceptance Rate at 0%, 0.0001%, and 0.001%. Original is a set of original iris images. Constant is a set of iris images whose noises are replaced with constant values (the mean value of non-masked region is chosen for each images).

	FAR (%)	Original FRR (%)	Constant Filling FRR (%)	Hallucinating Irises – FRR (%)
Segmented by CMU-1	0	16.56	7.04	5.83
	0.0001	7.7	6.77	4.7
	0.001	4.34	4.09	3.7
Segmented by Masek algorithm	0	8.45	7.4	6.99
	0.0001	8.45	7.4	6.99
	0.001	4.76	5.55	5.02

V. Conclusions

In this paper, we proposed a new approach to produce "hallucinated iris images" from partial occluded irises. We showed that the proposed algorithm can improve the performance of iris recognition by replacing occlusion regions with sample textures from a valid partial iris region. We can effectively reduce the effects of occlusion around masks and thus reduce the effects on the Gabor feature extraction around the boundary regions of the occlusions. Using the "Hallucinated Irises" generated in this paper and the results recorded suggest that other iris recognition algorithms with similar linear filtering approaches can also improve their performances by using the proposed algorithm.

From the experimental results shown in section IV, a few observations are worth noting. First, when looking at the recognition performance for the data segmented by CMU-1algorithm, there is a significant improvement in the verification accuracy when our proposed algorithm is applied (10% gain at lowest FAR).

Second, when we compared the results from the data generated by the two different segmentation schemes, we can see that our proposed method does not improve the verification rate too much in the case of Masek's segmentation. The reason for this is stated in section IV-C. Therefore, our proposed algorithm shows its full power only when the occlusion masks are correctly identified to provide a substantial improvement, otherwise only a small improvement is observed. If the masks are incorrect, the image-filling algorithm may end up filling the images with noisy information, and using occlusion masks which are inaccurate will indubitably lead to a lower verification performance which might result in an even lower recognition rate. However, even in such circumstances, our proposed algorithm enhances the recognition rate, compared to filling the occluded region with a constant value.

There is still significant room to improve our proposed algorithm. For example, in [4], the goal of image-filling is to remove some undesired object in the image and make the iris image look more natural. But in our case, the goal of image-filling is to enhance the recognition performance. Therefore, if we can use a different objective function in the candidate searching scheme, our proposed method may further enhance the recognition rate.

Another key factor is the accuracy of the iris mask. As stated above, the accuracy of the iris mask has the greatest impact to the success of the proposed algorithm to produce occlusion free iris images. We should further investigate how to generate more accurate iris masks which cover all the occlusions in iris images.

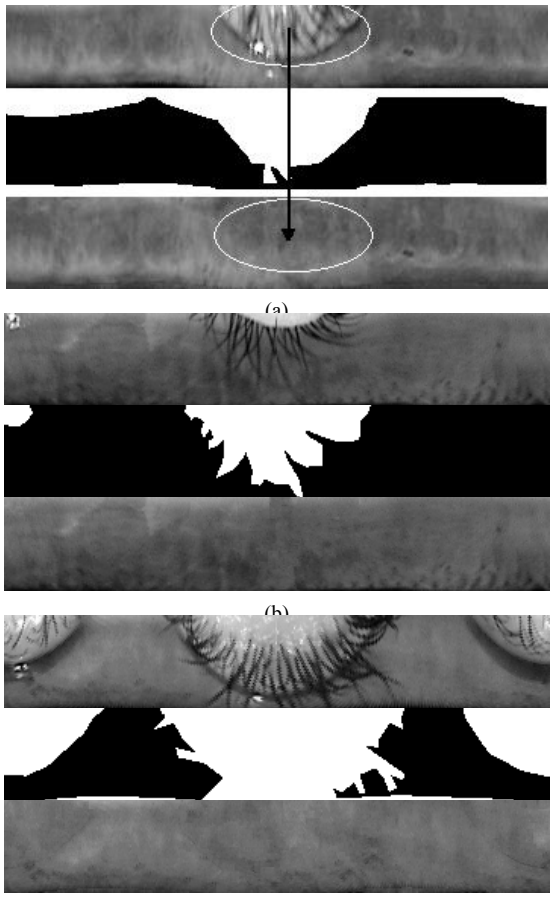

(c)

Fig. 7: Set of iris images in polar domain (segmented by CMU-1 algorithm). For each set of three images, the first image is an original image, the second image is a mask, and the third image is the "Hallucinated Iris" after the image-filling algorithm is applied.

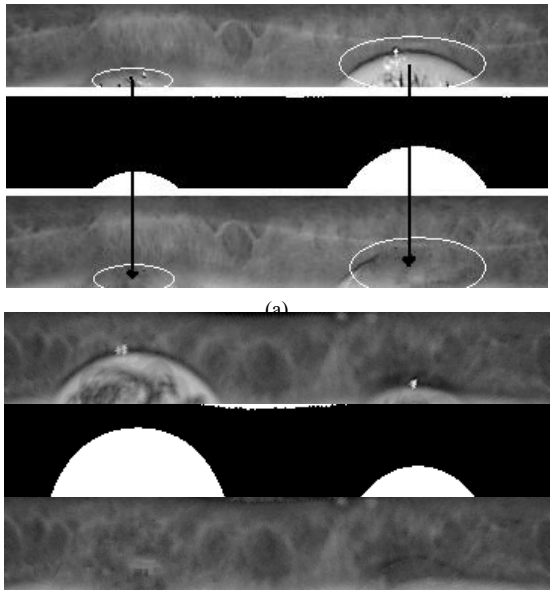

(b)

Fig. 8: Set of iris images in polar domain (segmented by Masek's algorithm). For each set of three images, the first image is an original image, the second image is a mask, and the third image is the resulting "Hallucinated Iris" after the image-filling algorithm is applied. In (a), we can see that the inaccurate mask causing the incorrect image filling results.

REFERENCES

[1] J. Daugman, "High Confidence Visual Recognition of Persons by a Test of Statistical Independence," *IEEE Trans. Pattern Analysis and Machine Intelligence*, Vol. 15, no. 11, pp. 1148-1161, Nov. 1993.

[2] R.P. Wildes, "Iris Recognition: An Emerging Biometric Technology," *Proc. IEEE*, Vol. 85, no.9, pp. 1348-1363, Sept. 1997.

[3] W. W. Boles, "A Security System Based on Human Iris Identification Using Wavelet Transform," *Proc. Int'l Conf. Knowledge-Based Intelligent Electronic Systems*, pp. 533-541, May 1997.

[4] A. Criminisi, P. P\érez, and K. Toyama, "Object removal by exemplar-based inpainting," in *Proc. Conf. Computer Vision and Pattern Recognition* Madison, WI, June 2003.

[5] W.K Kong and D.Zhang, "Accurate Iris Segmentation Based on Novel Reflection and Eyelash Detection Model," *Proc. Int'l Symposium on Intelligent Multimedia, Video and Speech Processing*, Hong Kong, pp.263-266 2001.

[6] J. Huang, Y. Wang, T. Tan and J. Cui, "Noise Removal and Impainting Model for IRIS Image," in *Proc. ICIP'04*, pp.869-872, 2004.

[7] P. Salama, N. Sharoff, E. J. Coyle and E. J. Delp, "Error concealment techniques for encoded video streams", In *Proc of* ICIP'95, pp.23-26,1995

[8] D. Zhang, D. M. Monro and S.Rakshit, "Eyelash Removal Method for Human Iris Recognition, *Proc. IEEE Int'l Conf. Image Processing*, pp. 285-288, Atlanta, Georgia, USA, Oct 8-11, 2006.

[9] L. Masek, "Recognition of Human Iris Pattern for Biometric Identification, "thesis, Univ. of Western Australia, http://www.csse.uwa.edu.au/pk/studentprojects/libor/,2003.

[10] "Iris Challenge Evaluation," National Institute of Standartds and Technology, http://iris.nist.gov/ICE/, 2006.

[11] J. Thornton, M. Savvides, and B.V.K. Vijaya Kumar, "Robust Iris Recognition Using Advanced Correlation Techniques," *Proc. Int'l Conf. Image Analysis and Recognition*, pp. 1098-1105,2005